



# Exploring the pharmacological and molecular mechanisms of *Salvia chinensis Benth* in colorectal cancer

### A network pharmacology and molecular docking study

Qian Zheng, MD<sup>a</sup>, Xin Wang, MD<sup>a,b</sup>, Tian Gao, MD<sup>a</sup>, Bingzhou Zhang, MD<sup>a</sup>, Ning Zhao, MD<sup>a</sup>, Runsen Du, MD<sup>a</sup>, Zengren Zhao, PhD<sup>a,\*</sup>

#### Abstract

While Salvia chinensis Benth (commonly known as "Shijianchuan" in Chinese, and abbreviated as SJC) is commonly used in adjuvant therapy for colorectal cancer (CRC) in traditional Chinese medicine, its mechanism of action remains unclear. In this study, Initially, we examined the impact of SJC on CRC cells in an in vitro setting. Next, we initially retrieved the primary active components and targets of SJC from databases such as TCMSP and existing literature. Subsequently, we integrated differential gene expression data from the GEO database and collected CRC-related targets from resources like DisGeNET. The matching of these datasets enabled the identification of SJC-CRC targets. We constructed a protein-protein interaction network and identified core targets through topological analysis. GO and KEGG enrichment analyses were performed using clusterProfiler. We established networks linking traditional Chinese medicine components to targets and core targets to signaling pathways. Additionally, we performed molecular docking to validate interactions between the main compounds and targets, and employed Western blot analysis to explore how the major components of SJC affect crucial signaling pathways. In this study, SJC inhibited the viability of HCT-116 and HT-29 cells. We identified a total of 11 active components in SJC along with 317 target genes. Among these, there were 8612 target genes associated with CRC, and we successfully matched 276 SJC-CRC target genes. Through topological analysis of the protein-protein interaction network, we pinpointed 20 core targets. It was revealed that SJC effects are linked to genes governing processes like cell apoptosis, proliferation, hypoxia, oxidative stress, and signaling pathways such as PI3K-Akt through GO and KEGG pathway enrichment analyses. Additionally, we applied molecular docking techniques and observed that the majority of active compounds displayed robust binding affinity with the selected targets. In vitro experiments suggested that SJC and its key component, Ursolic acid, may exert its anti-CRC effects by modulating the core PI3K/AKT signaling pathway through inhibiting the phosphorylation of the target Akt1. This discovery is consistent with the predictions derived from network pharmacology methods. This study marks the inaugural utilization of bioinformatics methods in conjunction with in vitro experiments to comprehensively investigate the pharmacological and molecular mechanisms responsible for SJC anti-CRC effects.

**Abbreviations:** CCK-8 = cell counting kit-8, CRC = colorectal cancer, DEGs = differentially expressed genes, DL = drug like, GEO = Gene Expression Omnibus, GO = gene ontology, KEGG = Kyoto encyclopedia of genes and genomes, OB = oral bioavailability, PPI = protein-protein interaction, SJC = *Salvia chinensis Benth* (commonly known as "Shijianchuan" in Chinese), TCM = traditional Chinese medicine, TCMID = Comprehensive Database of Traditional Chinese Medicine, TCMSP = Traditional Chinese Medicine Systems Pharmacology Database and Analysis Platform, UA = Ursolic acid.

Keywords: CRC, molecular docking, network pharmacology, PI3K/AKT signal pathway, Salvia chinensis Benth, Ursolic acid.

This study was supported partially by 2022 & 2023 Hebei introduction of foreign expert intelligence projects (YZ202201 & YZ2023), Hebei Natural Science Foundation (Nos. H2020206374 & H2021206306), National Natural Science Foundation of China (No.82203623) and Hebei clinical medicine excellent talents project of Province (No. LS202001).

The authors have no conflicts of interest to disclose.

All data generated or analyzed during this study are included in this published article [and its supplementary information files].

Our data was based on bioinformatics analysis and the data from TCMSP, TCMID, UniProt, GeneCards, String, Metascape, GO, and KEGG, so our study did not require the approval of an ethics committee.

Supplemental Digital Content is available for this article.

<sup>a</sup> Department of General Surgery, Hebei Key Laboratory of CRC Precision Diagnosis and Treatment, The First Hospital of Hebei Medical University, Shijiazhuang, China, <sup>b</sup> Department of Pathology, The First Hospital of Hebei Medical University, Shijiazhuang, China. \*Correspondence: Zengren Zhao, Department of General Surgery, Hebei Key Laboratory of CRC Precision Diagnosis and Treatment, The First Hospital of Hebei Medical University, Shijiazhuang 050000, China (e-mail: zhaozengren@hebmu.edu.cn).

Copyright © 2023 the Author(s). Published by Wolters Kluwer Health, Inc. This is an open-access article distributed under the terms of the Creative Commons Attribution-Non Commercial License 4.0 (CCBY-NC), where it is permissible to download, share, remix, transform, and buildup the work provided it is properly cited. The work cannot be used commercially without permission from the journal.

How to cite this article: Zheng Q, Wang X, Gao T, Zhang B, Zhao N, Du R, Zhao Z. Exploring the pharmacological and molecular mechanisms of Salvia chinensis Benth in colorectal cancer: A network pharmacology and molecular docking study. Medicine 2023;102:50(e36602).

Received: 18 September 2023 / Received in final form: 10 November 2023 / Accepted: 21 November 2023

http://dx.doi.org/10.1097/MD.0000000000036602

#### 1. Introduction

Colorectal cancer (CRC), as a prevalent malignancy within the digestive system, has consistently garnered significant global attention. According to data from the International Agency for Research on Cancer (IARC) of the World Health Organization (WHO) in 2020, there were approximately 1.932 million new cases of CRC worldwide, accounting for 9.8% of all new malignant tumor cases and ranking third. Furthermore, CRC was responsible for approximately 935,000 deaths, comprising 9.4% of all malignant tumor-related fatalities and ranking second.[1] Over the last 3 decades, the incidence of CRC in China has shown a consistent and increasing upward trend. According to Chinese official statistics in 2020, CRC had the secondhighest incidence rate and the fourth-highest mortality rate among malignant tumors.[2] While there have been some advancements in CRC treatment, a notable deficiency exists in researching the underlying treatment mechanisms. Urgent validation of these effects and the development of highly personalized treatment approaches are imperative.

Traditional Chinese medicine (TCM) has a rich history and unique advantages in the treatment of cancer, including supporting patients' immune systems, alleviating the adverse effects of radiation and chemotherapy, preventing recurrence and metastasis, improving the quality of life, and extending survival rates.[3] Salvia chinensis Benth (commonly known as "Shijianchuan" in Chinese, and abbreviated as SJC) is a frequently used herbal remedy in TCM for the treatment of gastrointestinal tumors. It is derived from the whole plant of the Lamiaceae family Salvia chinensis and is primarily found in the Jiangsu region of China. It has been documented in ancient TCM texts such as the "Ben Cao Gang Mu" and is known for its functions of clearing heat, detoxification, promoting blood circulation, and relieving pain. In clinical practice, it is commonly employed in the treatment of various malignant tumors, enteritis, dysentery, skin abscesses, and swellings. SJC, as a complex herbal remedy, demonstrates a multifaceted anticancer mechanism. Research suggests that SJC suppresses WT1 oncogene expression in liver cancer cells via the Wnt/β-catenin signaling pathway.[4] Prior studies have demonstrated that SJC induces autophagy in esophageal cancer cells by modulating the AMPK/ULK1 signaling pathway.<sup>[5]</sup> SJC polysaccharide components boost natural killer cell cytotoxicity against mouse liver cancer, inhibiting its progression. [6] Furthermore, Wang et al found that SJC aqueous extract inhibits the occurrence and development of triple-negative breast cancer through DNA damage-related pathways.[7] Various studies have reported the anti-CRC effects of the primary components of Salvia chinensis Benth, such as Ursolic acid, quercetin, and resveratrol. For instance, Ursolic acid has been documented to induce apoptosis and modulate autophagy in apoptosis-resistant CRC cells via the JNK pathway. [8] On the other hand, Quercetin exerts anti-inflammatory effects and inhibits AOM/DSS-induced CRC in mice. [9] Resveratrol possesses the capability to induce apoptosis in CRC cells.[10] Despite the extensive clinical utilization of SIC and its established effectiveness in adjuvant CRC treatment, there remains a deficiency in comprehensive and systematic laboratory research and reporting concerning the experimental investigations and molecular mechanisms that underlie the anti-CRC properties of SJC.

Network pharmacology is an interdisciplinary field that integrates knowledge from computer science, bioinformatics, pharmacology, and other disciplines.<sup>[11]</sup> Its primary focus is to investigate the interactions between drugs and various biological molecules such as molecules, genes, proteins, and cells within the human body, as well as the mechanisms of drug action.<sup>[12]</sup> Systems biology suggests that complex diseases, such as cancer, arise not only from single-gene mutations but also from the disruption of the equilibrium in biological network systems due to multiple gene mutations.<sup>[13]</sup> The goal of network pharmacology

is to investigate the equilibrium of biological networks.<sup>[14]</sup> This approach highlights the synergistic actions of various components, pathways, and targets, making it especially suitable for analyzing the effects of traditional Chinese medicine, helping identify therapeutic targets for drug active components, improving drug efficacy, and minimizing adverse reactions. It important to note that network pharmacology research methods are extensively used to investigate the mechanisms of action of various traditional Chinese medicines in CRC. These methods play a significant role in screening components and exploring component-target interactions.<sup>[15,16]</sup>

Molecular docking is a computer simulation technique that models interactions between molecules and proteins at the atomic level.<sup>[17]</sup> It predicts ligand and receptor conformations and calculates parameters, such as affinity, to evaluate binding interactions. This technology is accurate, cost-effective, and mainly employed in drug design and the elucidation of biochemical pathways.

In this study, we initially investigated the impact of SJC on CRC cells in vitro. Subsequently, we utilized bioinformatics approaches, including network pharmacology and molecular docking, to identify the crucial bioactive compounds, potential target genes, and signaling pathways associated with the therapeutic effects of SJC in CRC. Finally, at the cellular level, we employed Western blotting to explore the mechanistic actions of the primary components of SJC on core targets and pathways. These findings establish a basis for comprehending the mechanisms by which SJC aids in the adjuvant treatment of CRC. The research flowchart is described in Figure 1.

#### 2. Materials and methods

#### 2.1. Herbal extract preparation

Salvia chinensis Benth was provided by Sinopharm Le Ren Tang Pharmaceutical Co., LTD (Shijiazhuang, Hebei, China), and were subjected to a back-to-back identification of their physical characteristics and microscopic features by 2 experienced pharmacists in accordance with the pharmacopeial standards and traditional Chinese medicine processing specifications. The Chinese herbal materials were powdered, soaked in anhydrous ethanol overnight, and subsequently centrifuged to remove the residue. Bacteria were filtered using a 0.22 µm sterile filter membrane. The supernatant was gently evaporated using a rotary evaporator at low temperature until all anhydrous ethanol had evaporated. The resulting powder was collected and stored at -80°C for future use. Before the experiment, it was dissolved in DMSO to prepare a stock solution. The doses utilized in this study were expressed as the equivalent weight per milliliter of the original herbal material.

#### 2.2. Cell viability

HCT116 and HT29 cells were plated in 96-well plates at a density of  $3\times10^3$  cells per well and exposed to varying concentrations of SJC (0, 50, 100, 200, 300, and 400 µg/mL) or Ursolic acid (0, 5, 10, 20, 40, and 80 µM) for 24, 48, and 72 hours. Cell proliferation was evaluated using the cell counting kit-8 (CCK-8, Sigma–Aldrich, Shanghai, China) by measuring absorbance at a wavelength of 450 nm. Data analysis and graphical representation were carried out using GraphPad Prism 9.0 software.

#### 2.3. Construction of a database of main active components

To identify the active components in Salvia chinensis Benth, we employed 2 sources: the Traditional Chinese Medicine System Pharmacology Database and Analysis Platform (TCMSP, available at https://tcmspw.com/tcmsp.php)<sup>[18]</sup> and the Comprehensive Database of Traditional Chinese Medicine

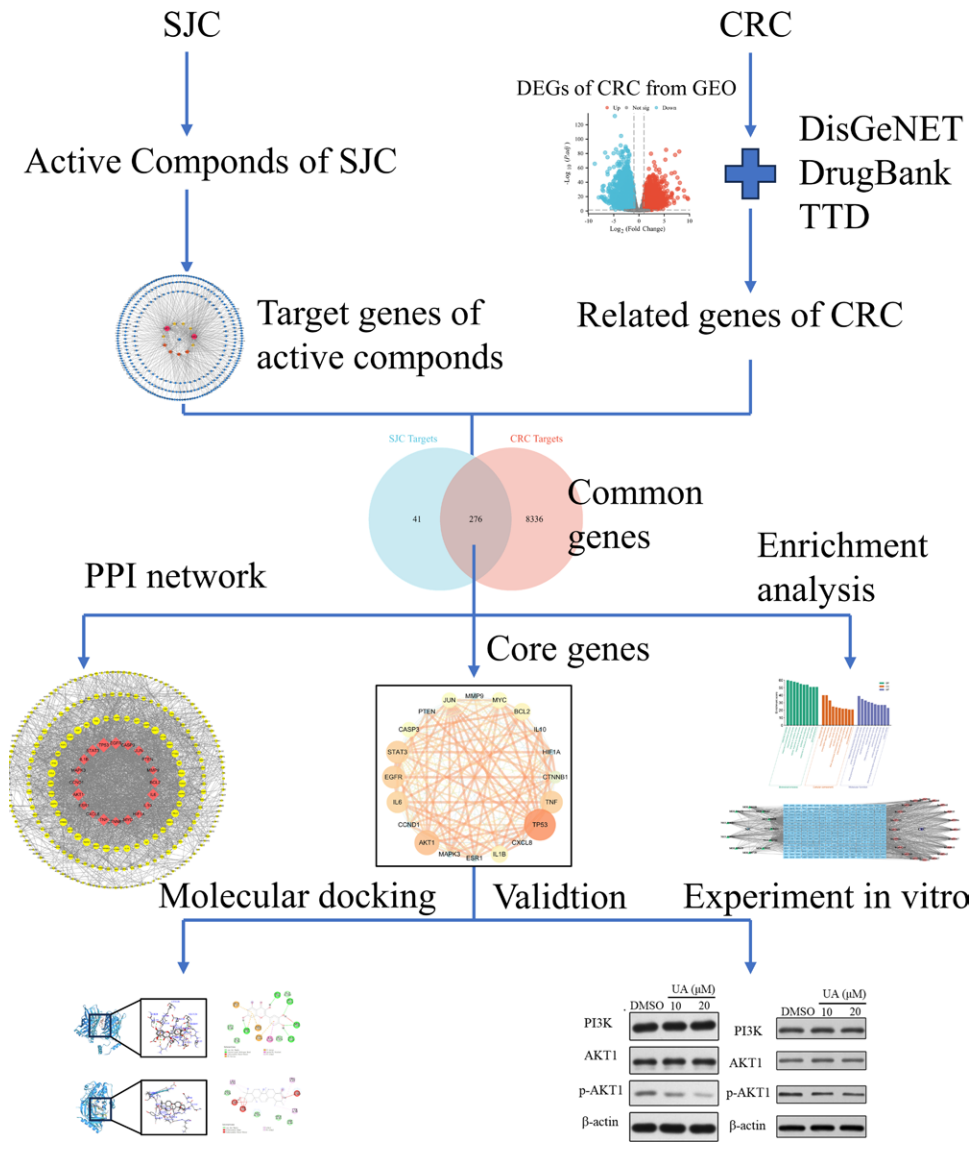


Figure 1. A flowchart of exploring the Pharmacological and Molecular Mechanisms of Salvia chinensis Benth in Colorectal Cancer.

(TCMID, available at https://119.3.41.228:8000/tcmid/). [19] We also gathered information for other compounds from the China National Knowledge Infrastructure (CNKI, available at https://www.cnki.net/) and PubMed (available at https://pubmed.ncbi.nlm.nih.gov/). Next, we applied toxicokinetic ADME criteria, as reported in the literature (OB  $\geq$  30%, DL  $\geq$  0.18), to select the primary active components. [20] Notably, compounds that did not meet these criteria were still considered if they had demonstrated efficacy against CRC in relevant literature (Supplementary Material Table S1, http://links.lww.com/MD/L84). To determine the molecular structures of these related compounds, we made use of PubChem (accessible at https://pubchem.ncbi.nlm.nih.gov/).

#### 2.4. Construction of potential targets of active components

The active components of a drug exert their biological effects through specific targets. To identify these targets for the core active components of SJC, we utilized the TCMSP database for direct target information. Additionally, we employed canonical SMILES number, a structural code, to aid in target identification. Several computational tools, including the Similarity Ensemble Approach (https://sea.bkslab.org/),<sup>[21]</sup> SwissTarget Prediction

(https://new.swisstargetprediction.ch/), [22] were leveraged to explore a wide array of potential targets for SJC.

#### 2.5. Construction of a CRC-related targets database

We initiated our study by procuring microarray data that contained differentially expressed mRNAs in the CRC tissues and their adjacent tissues, distinguishing between a CRC group and a normal group. We sourced this dataset from the GEO database, accessible at https://www.ncbi.nlm.nih.gov/ geo/, Series: GSE138202. We analyzed the mRNA expression data of CRC tissues and adjacent non-cancer tissues using the GEO2R software. Genes with an adjusted-P value < .05 and a log<sub>2</sub>|fold change| > 1 were considered significantly differentially expressed and deemed CRC-related targets. We used the ggplot2 package (version 3.3.6) in R software to generate a volcano plot for the differentially expressed genes (DEGs). In addition, we collected CRC-related disease targets from various databases, including the DisGeNET database (https://www.  $disgenet.org/web/DisGeNET/menu/home), \cite{Months} the \ \ DrugBank$ database (https://go.drugbank.com/),[24] TTD database (https:// db.idrblab.org/ttd/),[25] and Uniprot database (https://www.uniprot.org/), [26] using keywords such as "colorectal carcinoma" and "colorectal cancer." The data retrieved from the mentioned databases was combined with the differential expression genes (DEGs) acquired from the GEO database, resulting in a comprehensive CRC-related gene database, with duplicate entries duly removed.

#### 2.6. Construction of the PPI network

Following the aforementioned analyses, we cross-referenced the target of the core active ingredient in SJC with the disease target specific to CRC. This intersection yielded the compound target of SJC-CRC. To visually represent this overlap, we generated a VENN diagram using the ggplot2 and VennDiagram tools. Additionally, we constructed a protein-protein interaction (PPI) network for these targets using the String database, accessible at https://string-db.org/.<sup>[27]</sup>

## 2.7. Construction of the "Herbs-components-targets" network of SJC

Based on the previously obtained PPI network, we proceeded to construct the "Herbs-Components-Targets" network (H-C-T network) of SJC using Cytoscape 3.9.1. Within this network, we applied a rigorous screening process based on the topological characteristics of the network. Specifically, we focused on 3 key parameters: Degree Centrality (DC), Closeness Centrality (CC), and Betweenness Centrality (BC). Degree centrality, a measure of how many connections a node has within the network, was used to assess the importance of each node. Nodes with higher degree centrality were considered more critical. Betweenness centrality, on the other hand, quantified the number of shortest paths that passed through a given node, indicating its intermediary centrality. Lastly, closeness centrality evaluated the total distances from a node to all others in the network, with smaller sums indicating greater proximity to other nodes. To identify core composite targets within SJC, we set specific criteria. Targets with a degree centrality exceeding twice the median value were selected. Meanwhile, for betweenness centrality and closeness centrality, targets with values equal to the median were chosen. This selection process aimed to pinpoint the most influential and critical nodes in the network, aligning with the criteria established in relevant literature reports.

#### 2.8. GO and KEGG enrichment analysis

Following the identification of the core targets, we employed clusterProfiler (version 4.4.4) for the purpose of conducting GO and KEGG enrichment analyses. These analyses were carried out with a stringent criterion, setting the false discovery rate (FDR) threshold to be <0.05.

The GO enrichment analysis provided insights into the biological processes, cellular components, and molecular functions associated with the core targets. In parallel, the KEGG (Kyoto Encyclopedia of Genes and Genomes) enrichment analysis delved into potential biological pathways and functional annotations linked to these targets. The outcomes of these analyses were visually represented using bubble plots, generated through the ggplot2 package.

#### 2.9. Active components-targets docking

To assess the accuracy of the main components and their predicted targets, we selected 9 components from the core components of SJC and performed docking simulations with 9 proteins chosen from the core targets.

For this purpose, we obtained the candidate compositions and the crystal structures of the target proteins from the PubChem database (https://pubchem.ncbi.nlm.nih.gov/) and RCSB Protein Data Bank (https://www.pdb.org/), respectively. We preferred target protein models with ligand binding sites smaller than 3Å for enhanced precision.

The following steps were undertaken:

- i) Preprocessing of Protein Structures: The protein crystal structures were imported into AutoDockTools 1.5.7 Software for preparation. This involved tasks such as dehydrating, hydrogenating, and separating the ligands from the protein structures.
- ii) Grid Box Setup: Using AutoDockTools 1.5.7, a docking grid box was constructed for each target protein to define the search space for the docking simulations.
- iii) Docking Simulations: The actual docking simulations were carried out using AutoDock4. These simulations allowed the molecules from SJC to interact with the target proteins within the defined grid boxes.
- iv) Selection of Docking Conformations: After docking, the molecules with the lowest binding energy in the docking conformation were selected for further analysis.
- v) Binding Analysis: The selected conformations were analyzed to observe the binding effects, including comparisons with the original ligands and assessment of various intermolecular interactions, such as hydrophobic interactions, cation-π interactions, anion-π interactions, π-π stacking, and hydrogen bonding.

#### 2.10. Western blot analysis

Protein lysates were extracted from cells using radioimmunoprecipitation assay buffer (Beyotime, Shanghai, China), and total protein was collected by centrifugation at 12,000 x g and 4°C for 15 minutes. Proteins were separated through sodium dodecyl sulfate-polyacrylamide gel electrophoresis (SDS-PAGE) and subsequently transferred onto polyvinylidene fluoride membranes (Millipore, Bedford, MA, USA). Following blocking with 5% bovine serum albumin (Gen-view Scientific Inc., USA) at room temperature for 1.5 hours, the membranes were then incubated overnight at 4°C with primary antibodies against 3-phosphoglycerate dehydrogenase (Abclonal, Wuhan, Hubei, China), PI3K (Abcam Technology, Cambridge, MA, USA), AKT1 (Santa Cruz Biotechnology, Dallas, TX, USA), p-AKT1 (CST, Littleton, CO, USA), and β-actin (Abcam Technology, Cambridge, MA, USA). The antibody was diluted in the ratio of 1:1000. Subsequently, the membranes were incubated with secondary antibodies conjugated to horseradish peroxidase (ProteinTech) at room temperature for 1 hour. Protein bands were detected and visualized using an enhanced chemiluminescence detection kit (New Cell & Molecular Biotech, Shanghai, China).

#### 2.11. Statistical analysis

The data is presented as the mean  $\pm$  standard deviation (SD). Unpaired 2-tailed t-tests were performed using GraphPad Prism 9.0. A P value of < .05 was considered as statistically significant.

#### 3. Results

#### 3.1. SJC inhibited the viability of CRC cells

CCK-8 experiments were conducted to investigate the in vitro cytotoxicity of SJC on human CRC cell lines (HCT-116, HT-29). Figure 2A and B illustrated the time-dependent and dose-dependent inhibitory effects of SJC on CRC cells. These results suggested that SJC demonstrated anti-tumor cytotoxicity against CRC cells.

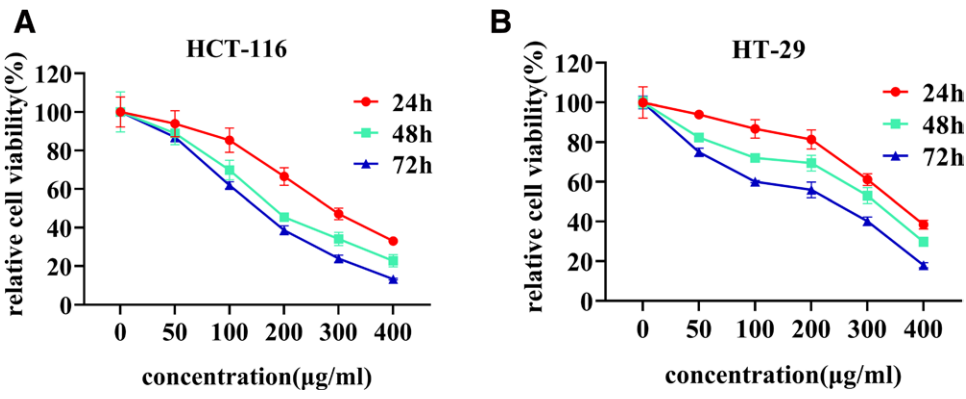


Figure 2. SJC inhibits the viability of CRC cells as measured by the CCK8 assay. (A) HCT116, (B) HT29 cells were treated with various concentrations of quercetin for 24, 48, and 72 h, respectively. Data are presented as the mean ± SD from at least 3 independent experiments. CRC = colorectal cancer.

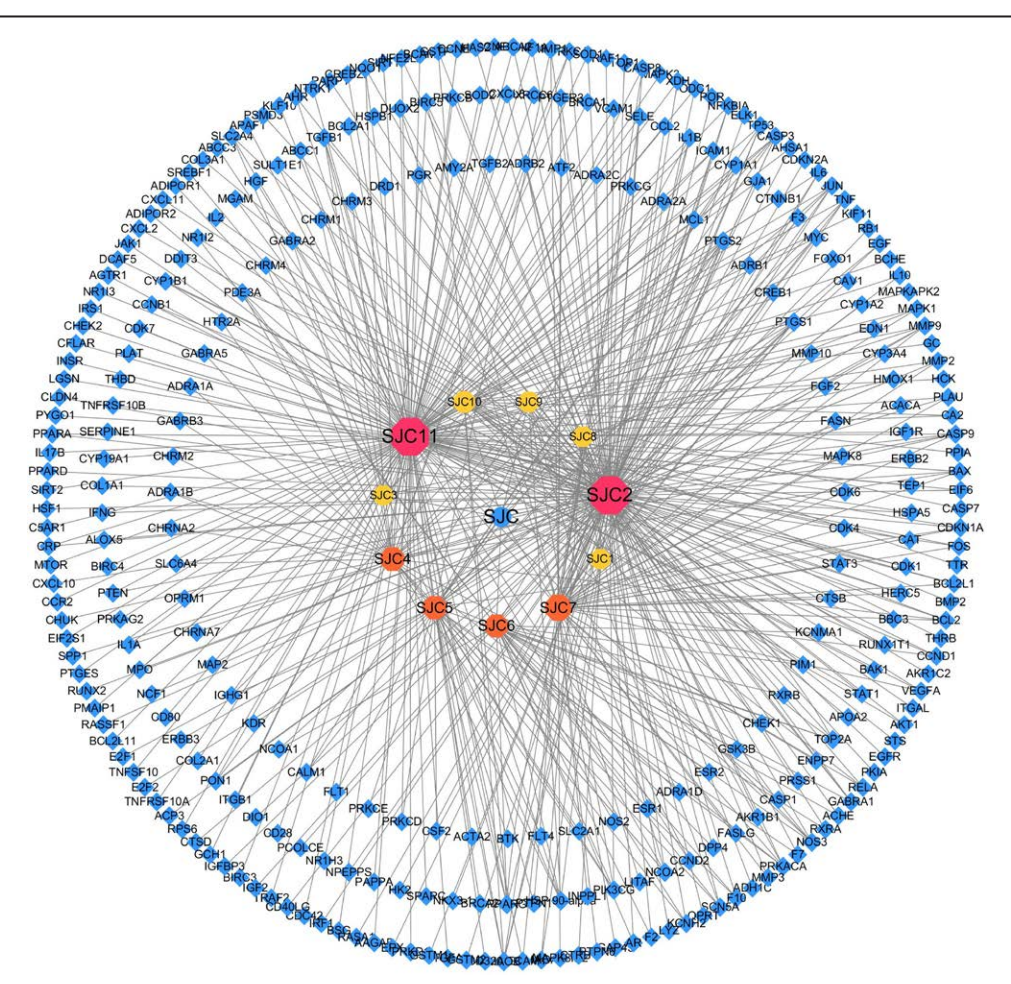


Figure 3. Herb-compound-target network. The central blue circle represents Chinese herbal medicine SJC, the surrounding regular octagon signifies the active components of SJC, and the outer blue diamonds symbolize the target proteins of these active components. The edges represent the interaction between compounds and targets, and the node size is proportional to the degree of interaction.

## 3.2. Analysis of the bioactive compounds in SJC and their potential targets

We have successfully identified a total of 11 bioactive compounds within SJC, drawing data from the TCMID and TCMSP databases, as well as pertinent literature sources (Supplementary Material Table S1, http://links.lww.com/MD/L84). To unveil the potential targets for these 11 active compounds in SJC, we harnessed the TCMSP target module. Subsequently, these targets were converted into gene symbols, leveraging the comprehensive

UniProt database. Armed with this information, we embarked on the creation of an herb-compound-target network within Cytoscape 3.9.1. This network, an intricate web comprising 329 nodes and 530 edges (Fig. 3, Supplementary Material Table S2, http://links.lww.com/MD/L85), offered valuable insights into the intricate and multifaceted effects of the active compounds found in SJC.

Our network analysis illuminated the significance of these compounds, ranked in descending order of degree centrality as follows: Quercetin (degree: 155), Resveratrol (degree: 152),

Ursolic acid (degree: 56), Beta-sitosterol (degree: 38), Emodin (degree: 36), Deoxyschizandrin A (degree: 31), Daucosterol (degree: 21), Chrysophanol (degree: 13), Vanillin (degree: 11), Caffeic acid (degree: 10), Oleanolic acid (degree: 7). Degree centrality, as a pivotal metric within this context, underscores the significance of these chemical components in their influence on SJC. Notably, higher degree values correspond to more pronounced and impactful effects.

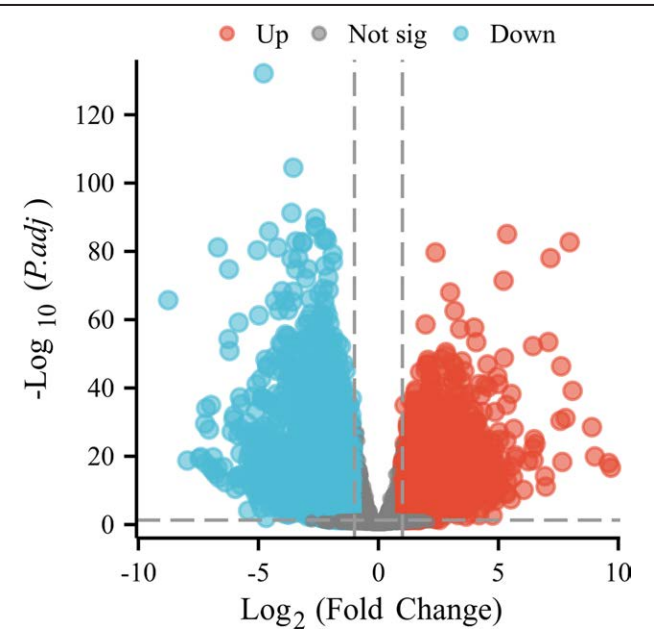


**Figure 4.** The volcano plot illustrates the distribution of differentially expressed genes in the disease samples obtained from the GEO database. Red and blue colors indicate upregulated and downregulated genes, respectively, while black signifies no significant difference. GEO = Gene Expression Omnibus.

#### 3.3. Analysis and acquisition of targets in CRC

We procured transcriptome data derived from a collection of CRC and adjacent normal tissue samples contained within the GEO database, specifically from dataset GSE138202. Through rigorous analysis facilitated by the GEO2R software, we unveiled a substantial pool of 8883 differentially expressed genes (DEGs) (Fig. 4, Supplementary Material Table S3, http://links.lww.com/MD/L86). Among these, 4298 genes were found to be upregulated, while 4585 genes exhibited downregulation in CRC. Furthermore, we embarked on the integration of disease targets pertinent to CRC. Our approach involved meticulous curation and the elimination of duplicate values originating from various sources, including DEGs from GEO, OMIM, TTD, and GeneCards. The outcome of this rigorous process yielded a collection of disease targets specifically linked to CRC, detailed in Supplementary Material Table S4, http://links. lww.com/MD/L87.

#### 3.4. Protein-protein interaction for anti-CRC with SJC

The intersection of targets associated with active compounds within SJC and the disease targets specific to CRC culminated in the identification of 276 common targets. These common targets were deemed pivotal in evaluating the anti-CRC activity of SJC compounds, as depicted in Figure 5 and outlined in Supplementary Material Table S5, http://links.lww.com/MD/L88.

To delve into the mechanisms underlying SJC anti-CRC effects, we initiated the construction of a protein-protein interaction (PPI) network by inputting the SJC-CRC key targets into STRING. This step was instrumental in filtering out unconnected targets, leading to the emergence of a robust PPI network. NetworkAnalyzer, a tool within Cytoscape 3.9.1, revealed that this network comprised 254 nodes and 2516 edges (Fig. 6A, Supplementary Material Table S6, http://links.lww.com/MD/L89). Notably, the median values for degree centrality (DC), closeness centrality (CC), and betweenness

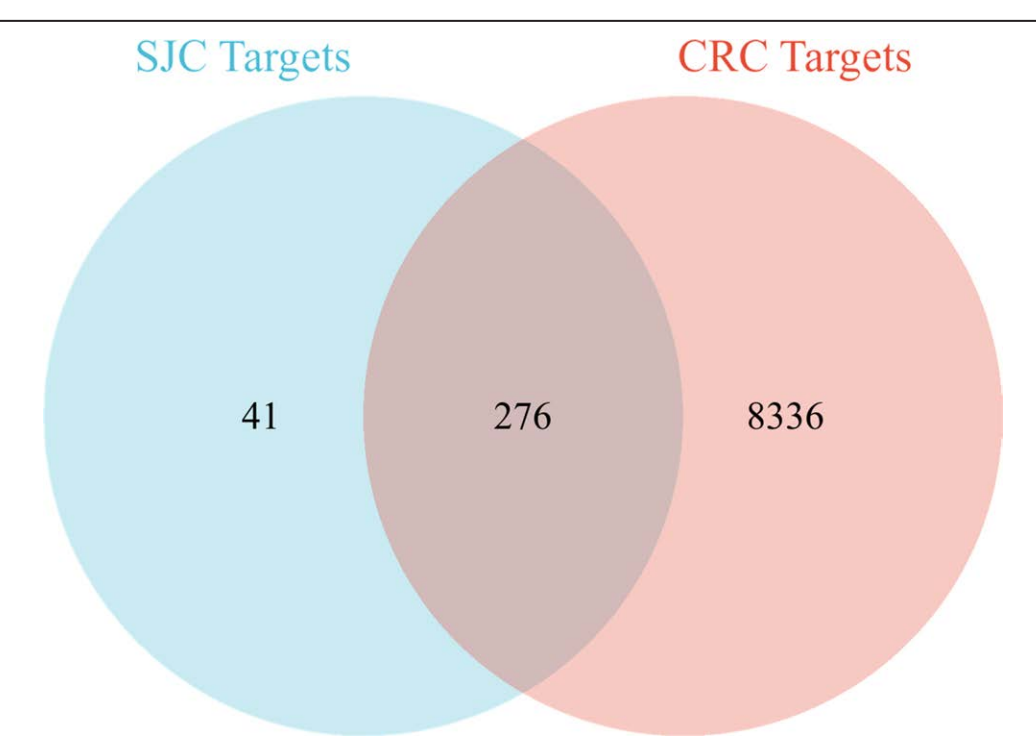


Figure 5. A Venn diagram illustrating the 276 common targets between the active compound targets of SJC and the disease targets of CRC. CRC = colorectal cancer.

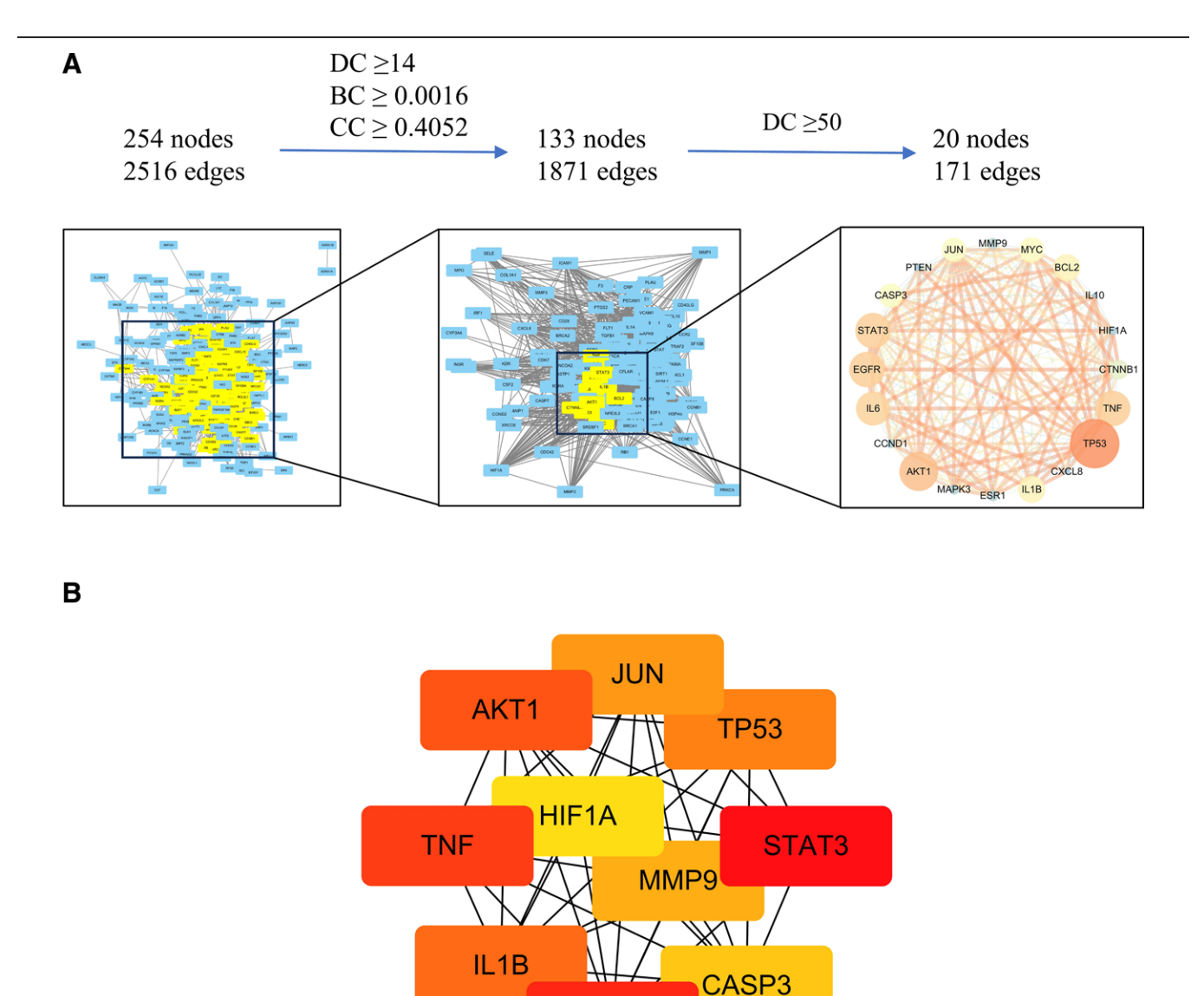


Figure 6. Identification of candidate targets via protein–protein interaction (PPI) analysis. (A) The process of topological screening for the PPI network. The 20 core targets were obtained by screening 111 common targets through DC, BC, CC; (B) The hub genes were selected from the PPI network using the CytoHubba plugin. The node color was from pale yellow to red, and the corresponding degree gradually larger.

IL<sub>6</sub>

centrality (BC) were measured at 14, 0.0016, and 0.4052, respectively. Employing network topology analysis, with a stringent screening criterion of DC  $\geq$  50, we discerned a core PPI network encompassing 20 pivotal targets. These core targets included TP53, AKT1, TNF, STAT3, EGFR, IL6, IL1B, BCL2, MYC, CASP3, JUN, CTNNB1, ESR1, MMP9, MAPK3, CCND1, HIF1A, PTEN, CXCL8, and IL10, as depicted in Figure 6A and detailed in Table 1. Moreover, we identified the top 10 hub genes utilizing the MCC (Maximum Clique Centrality) method with the CytoHubba plugin (Fig. 6B). We constructed a network illustrating interactions between core and non-core targets (Fig. 7A), where node size corresponds to the degree centrality value, indicating that larger nodes have higher degree centrality. Lastly, cluster analysis was performed using the MCODE algorithm to obtain a highly connected subnetwork. Targets were ranked based on the score, and the top 4 distinct groups are listed in Figure 7B. These comprehensive analyses served to illuminate the intricate interplay of key targets and potential mechanisms underpinning SJC anti-CRC effects.

#### 3.5. GO enrichment analysis

To further explore the mechanism of SJC against CRC, we conducted Gene Ontology (GO) enrichment analysis using the clusterProfiler package on the SJC-CRC intersection genes, which revealed 271 common targets participating in various aspects of cellular composition, biological processes (BP), molecular functions (MF), and cellular components (CC). The analysis yielded a total of 3053 enriched items across 3 categories: 2785 in BP, 190 in MF, and 78 in CC, each with an adjusted-P value of <.05 as the significance threshold (Supplementary Material Table S7, http://links.lww.com/MD/ L90). We visualized the top 20 enriched terms for Biological Processes (BP), Molecular Functions (MF), and Cellular Components (CC) using bubble plots (Fig. 8A-C), offering a clear overview of the most relevant terms. Furthermore, bar plots were used to display the top 10 terms in each category based on gene count (Fig. 8D). In terms of molecular function, the treatment of CRC with SJC primarily involved the regulation of processes such as DNA-binding transcription factor binding, protein serine/threonine/tyrosine kinase

Table 1
Information of 20 core targets.

No.	Gene symbol	Protein name	Degree
1	TP53	Cellular tumor antigen p53	104
2	AKT1	threonine-protein kinase	89
3	TNF	Tumor necrosis factor	84
4	STAT3	Signal transducer and activator of transcription 3	84
5	EGFR	Epidermal growth factor receptor	84
6	IL6	Interleukin-6	82
7	IL1B	Interleukin-1 beta	72
8	BCL2	Apoptosis regulator Bcl-2	72
9	MYC	Myc proto-oncogene protein	69
10	CASP3	Caspase-3	68
11	JUN	Transcription factor Jun	68
12	CTN-	Catenin beta-1	64
	NB1		
13	ESR1	Ethylene-responsive transcription factor ESR1	56
14	MMP9	Matrix metalloproteinase-9	56
15	MAPK3	MAP kinase-activated protein kinase 3	55
16	CCND1	G1/S-specific cyclin-D1	54
17	HIF1A	Hypoxia-inducible factor 1-alpha	54
18	PTEN	Phosphatidylinositol 3,4,5-trisphosphate 3-phosphatase	52
		and dual-specificity protein phosphatase PTEN	
19	CXCL8	C-X-C motif chemokine 8	51
20	IL10	Interleukin-10	50

activity, RNA polymerase II-specific DNA-binding transcription factor binding, signaling receptor activator activity, and receptor-ligand activity, among others. The biological processes chiefly included responses to peptides, responses to extracellular stimuli, responses to nutrient levels, responses to oxidative stress, and cellular responses to chemical stress. Additionally, the cellular components encompassed terms like membrane raft, membrane microdomain, transcription regulator complex, vesicle lumen, and cytoplasmic vesicle lumen. These enrichments offered valuable insights into the multifaceted mechanisms underlying the efficacy of SJC in CRC treatment.

#### 3.6. KEGG enrichment analysis

We conducted a rigorous KEGG pathway enrichment analysis on the 276 SJC-CRC intersection targets utilizing the clusterProfiler package, with a significance threshold set at an adjusted-*P* value of <.05. This comprehensive analysis revealed a high level of enrichment across 187 pathways, as detailed in Supplementary Material Table S8, http://links.lww.com/MD/L91.

Based on gene counts, the top 20 KEGG pathways have been visually presented in Figure 9A. Among the prominent pathways were the PI3K-Akt signaling pathway, Lipid and atherosclerosis pathway, Human cytomegalovirus infection pathway, MAPK signaling pathway, and Kaposi sarcoma-associated herpesvirus infection pathway, among others.

To offer a holistic view of the interactions between targets, compounds, and pathways, we meticulously selected the top 20 pathways based on gene ratios, adjusted-*P* values, and their associated targets and compounds. This informed the creation of a compound-target-pathway (CTP) network, a complex web comprising 339 nodes and 1378 edges, meticulously crafted using Cytoscape 3.9.1 (Fig. 9B).

To further visualize the relationship between the top 9 genes from the core network and the top 20 signaling pathways, a Sankey diagram was thoughtfully generated. This diagram, realized through ggalluvial (version 0.12.3) and ggplot2, offered an insightful and comprehensible representation of these intricate relationships, as showcased in Figure 9C.

#### 3.7. Components-targets docking analysis

To corroborate the findings of network pharmacology, we conducted molecular docking evaluations involving selected active compounds and targets. Guided by degree centrality ranking, we identified the top 9 core targets (AKT1, TP53, EGFR, STAT3, TNF, IL6, BCL2, IL1B, and MYC) in the PPI network of SJC-CRC intersection targets and the top 9 compounds (Quercetin, Resveratrol, Ursolic acid, Beta-sitosterol, Emodin, Deoxyschizandrin A, Daucosterol, Chrysophanol, and Vanillin) in the herbal compound-target network for molecular docking analysis.

We obtained the crystal structures of core target proteins from the RCSB Protein Data Bank, and we retrieved the molecular structures of compounds from the PubChem database. The spatial coordinates for docking and comprehensive information about the proteins are provided in Table 2. The binding energies of the key targets and active compounds were presented in the form of a heatmap (kcal/mol) (Fig. 10). The computed free binding energies of the docking results fell within the range of –2.88 to –8.3 kcal/mol. Typically, binding energies less than –4.25 kcal/mol, –5.0 kcal/mol, or –7.0 kcal/mol are indicative of certain, good, or strong binding activity between the ligand and the receptor, respectively. [28,29]

The compounds with the highest binding free energy scores and their respective binding modes of interaction were visualized using Autodock 1.2.7 and Discovery Studio 2020 (Fig. 11A–I). For example, the free binding energy of Ursolic acid with AKT1 was 8.3 kcal/mol. This binding affinity was attributed to hydrogen bonding with GLU-124, GLU-111, GLU-95, ASP-19 and ARG-109 residues, van der Waals forces with LEU-18, SER-28, GLU-124 and ALA-110 residues, cation-π and anion-π interactions with ARG-122, ARG-109, and GLU-17 residues of AKT1, as well as hydrophobic interactions with ILE-123 (Fig. 11A).

Furthermore, hydrogen bonding, cation- $\pi$  interactions, anion- $\pi$  interactions, and hydrophobic interactions between small molecules and active cavities of target proteins led to the formation of stable complexes. Notably, quercetin, resveratrol, Ursolic acid, and beta-sitosterol exhibited strong binding activity with TP53, EGFR, STAT3, TNF, and MYC in this study. Hence, these compounds emerge as potential drug candidates.

It is essential to underscore that, although molecular docking offers valuable insights into the binding interactions between compounds of SJC and potential CRC-related targets, experimental validation is imperative to confirm the potential therapeutic properties of these herbal compounds.

#### 3.8. Ursolic acid inhibited the viability of CRC cells

To further elucidate the mechanism underlying SJC anti-CRC effects, we examined the influence of SJC primary active components on CRC cells. CCK-8 assays were conducted to assess the anticancer effects of Ursolic acid on HCT116 and HT29 cells at varying concentrations (0, 5, 10, 20, 40, and 80  $\mu M$ ) and time intervals (24, 48, and 72 hours). As depicted in Figure 12A and B, Ursolic acid markedly decreased the viability of HCT116 and HT29 cells in a manner dependent on both dose and time.

## 3.9. Ursolic acid inhibited the PI3K/AKT pathway in CRC cells

KEGG pathway enrichment analysis indicated that SJC predominantly modulated the PI3K/AKT pathway during the inhibition of CRC. Molecular docking results demonstrated strong binding affinity between Ursolic acid and the AKT1 protein. To delve deeper into the molecular mechanisms by which Ursolic acid participates in inhibiting HCT116 and HT29 cells in the context of its anti-CRC effects, we examined the relationship between Ursolic acid and the core PI3K/AKT

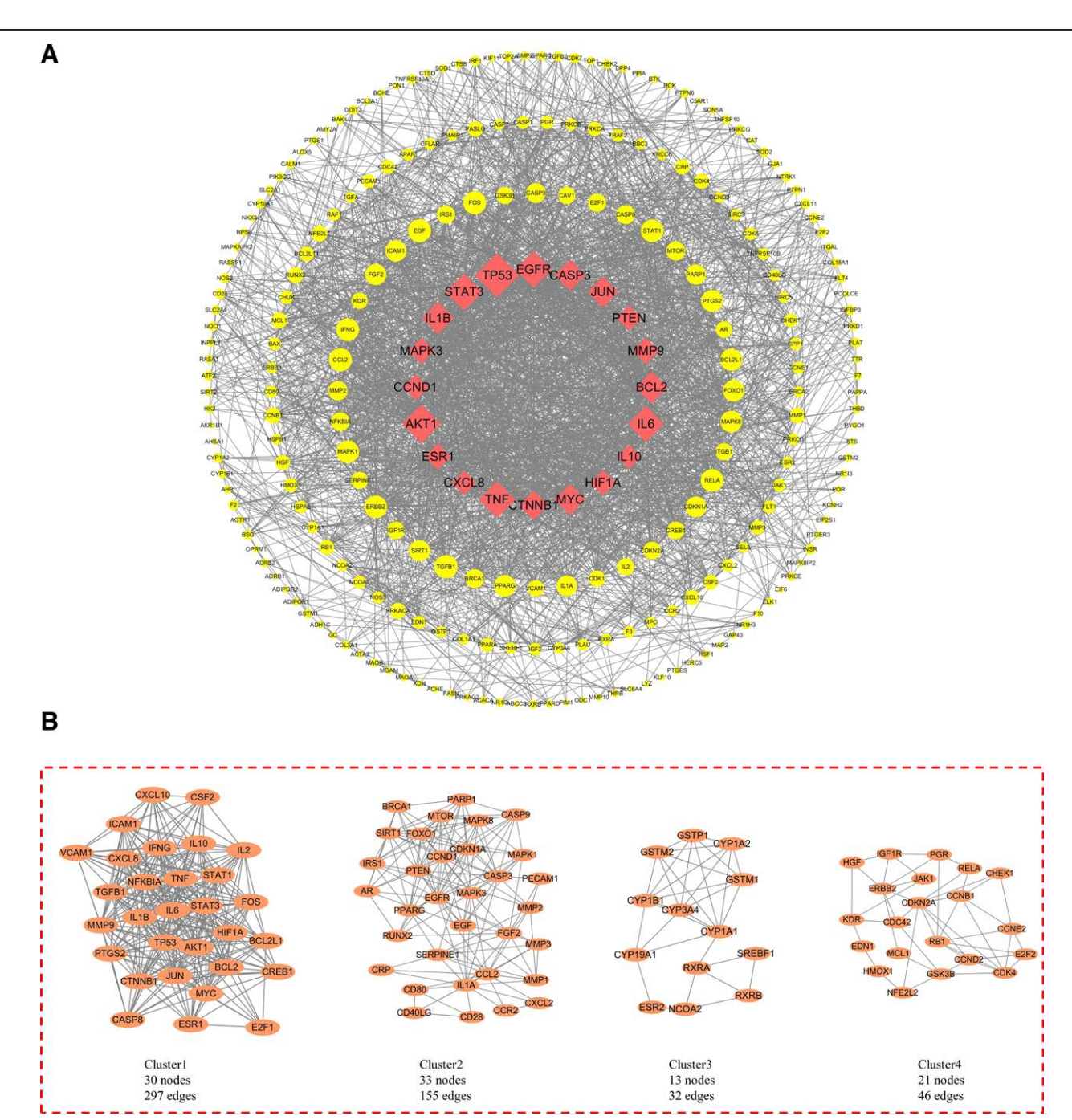


Figure 7. Analysis of the regulatory and clustering of core genes among the common genes in SJC-CRC. (A) the core targets and non-core targets network. The red diamond node nodes represent the core targets of SJC-CRC, the node size is proportional to the target degree in the network; (B) PPI network based on clustery analysis using the MCODE plug-in. CRC = colorectal cancer.

pathway through Western blotting analysis. As illustrated in Figure 12C–F, the levels of p-AKT1 protein significantly decreased in a dose-dependent manner. However, alterations in the levels of PI3K and AKT1 proteins were not statistically significant. These findings suggested that Ursolic acid may inhibit HCT116 and HT29 cells by suppressing the activity of the PI3K/AKT pathway.

#### 3.10. SJC inhibited the PI3K/AKT pathway in CRC cells

To further investigate the molecular mechanisms underlying SJC inhibition of HCT116 and HT29 cells, we conducted Western blotting analysis to study the relationship between SJC extract and the PI3K/AKT pathway. The Western blot results

demonstrated a significant reduction in the protein expression levels of p-AKT1 following SJC treatment (Supplementary Material Figure A–D, http://links.lww.com/MD/L83). In comparison to the control group, no statistically significant alterations were observed in the protein expression levels of PI3K and AKT1. These results substantiated the potential of SJC to suppress HCT116 and HT29 cells by inhibiting the PI3K/AKT pathway.

#### 4. Discussion

Colorectal cancer is on the rise globally, and its development is closely associated with factors like genetics, dietary habits, and lifestyle choices.<sup>[30]</sup> In the past, CRC was predominantly

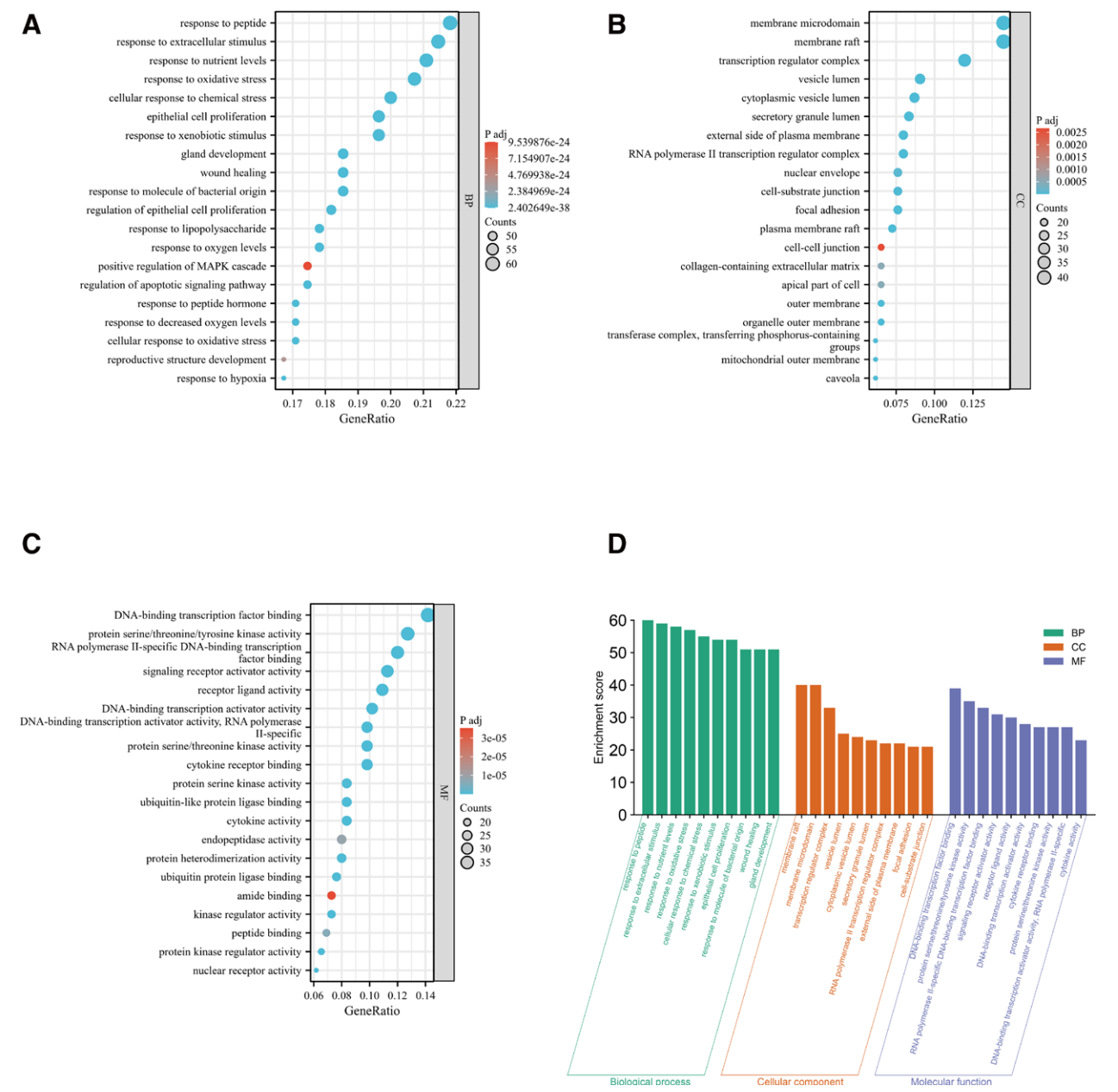


**Figure 8.** Results of GO enrichment analysis. (A) Bubble chart displaying biological process categories in GO enrichment analysis; (B) Bubble chart displaying biological process categories in GO enrichment analysis; (C) Bubble chart depicting molecular function categories in GO enrichment analysis; The x-axis and y-axis indicate the gene ratio and the full name of each process. The color and size of each bubble represent the *P* value and gene count. Subsequent bubble charts follow a similar format. (D) The top 10 categories for biological processes (BP), cellular components (CC), and molecular functions (MF) in GO enrichment analysis are presented as green, orange, and purple bar graphs, respectively.

associated with Western developed nations characterized by high-fat, low-fiber diets. However, with the economic growth of developing countries like China, Westernized dietary habits, combined with factors such as reduced physical activity and increased obesity rates, have contributed to a gradual rise in CRC cases.<sup>[31]</sup> This concerning trend now affects younger individuals and imposes significant societal and economic burdens on developing nations. Colorectal cancer often develops silently, with most cases originating from adenomas. Reports indicate that at the time of diagnosis, 50% of cases have already undergone malignant tumor metastasis, commonly affecting the liver and lungs.<sup>[32]</sup> The current treatment modalities for CRC encompass surgery, chemotherapy, radiation therapy, immunotherapy, and targeted therapy. Despite advancements in surgical techniques, radiochemotherapy, and updates in immunotherapy

and targeted therapy drugs, both the incidence and mortality rates of CRC persistently increase. These medical techniques can be accompanied by side effects, such as impaired liver and kidney function following radiation therapy or chemotherapy, decreased gastrointestinal function, compromised immune system, and heightened pain, among others.<sup>[33]</sup>

With a history of over 2000 years in China and the broader Asian region, Traditional Chinese Medicine (TCM) has unique advantages in cancer treatment. Several Chinese herbal medicines, whether used individually or in conjunction with radiation and chemotherapy, have demonstrated promising anti-CRC effects while causing fewer side effects. [34] Salvia chinensis Benth (SJC) has been utilized in the treatment of various cancers, exhibiting particularly favorable results in clinical practice for CRC. Our preliminary studies have indicated that in vitro, SJC

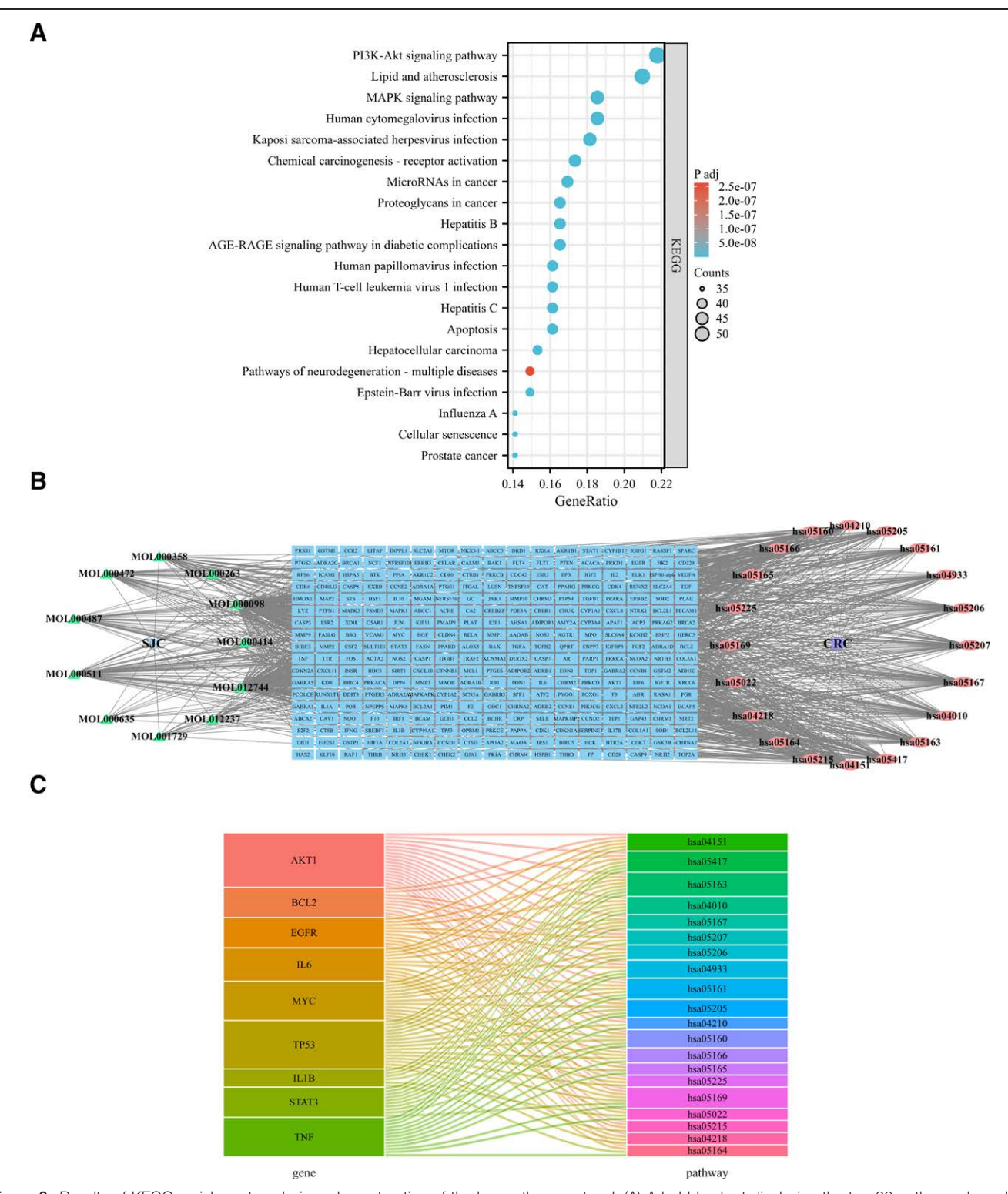


Figure 9. Results of KEGG enrichment analysis and construction of the key pathway network.(A) A bubble chart displaying the top 20 pathways based on KEGG enrichment analysis; (B) The compound–target–pathway network illustrating the mechanism of SJC in CRC treatment. Blue rectangles represent targets, green triangles represent compounds, and red ellipses represent pathways; (C) A sankey diagram depicting the KEGG pathway analysis of therapeutic targets in SJC CRC treatment. The left rectangle nodes represent the top 9 core therapeutic targets, the right rectangle nodes represent the top 20 KEGG pathways, and the lines in between depict the relationships between targets and pathways. CRC = colorectal cancer. KEGG = Kyoto encyclopedia of genes and genomes.

displays a dose- and time-dependent inhibitory effect on human CRC cells. The primary objective of this study is to investigate the potential mechanisms underlying SJC treatment of CRC.

We collected 11 chemical components from the TCMSP database, including major active components such as Quercetin (degree: 155), Resveratrol (degree: 152), Ursolic

acid (degree: 56), Beta-sitosterol (degree: 38), Emodin (degree: 36), Deoxyschizandrin A (degree: 31), Daucosterol (degree: 21), Chrysophanol (degree: 13), Vanillin (degree: 11), Caffeic acid (degree: 10), and Oleanolic acid (degree: 7). These active components can form a robust interaction network. Among the predicted active components, Quercetin, Resveratrol, Ursolic

acid, Beta-sitosterol, and others have demonstrated favorable therapeutic effects on CRC. For instance, Quercetin can reduce oxidative stress markers like lipid peroxidation (LPO), nitric oxide (NO), superoxide dismutase (SOD), glucose-6phosphate dehydrogenase (G6PD), and glutathione (GSH) in the intestinal tissues of CRC mice. [9] This leads to improved inflammation and mucosal barrier function in the mouse intestine, ultimately exerting inhibitory effects on CRC. There are reports suggesting that Resveratrol can promote apoptosis in CRC cells by regulating β1-Integrin. [35] Additionally, Zheng et al found that Ursolic acid induces caspasedependent apoptosis in CRC cells and leads to apoptotic loss of the FAK/PI3K/AKT signaling axis and EMT-related pathways.[36] Furthermore, Wang et al demonstrated that the combined use of OXA and Beta-sitosterol has a synergistic tumor-inhibiting effect in a mouse xenograft model.[37] Moreover, Beta-sitosterol can mediate the p53/NF-κB/BCRP signaling axis to enhance CRC resistance to OXA chemotherapy. Additionally, other chemical components and their derivatives such as Emodin, Deoxyschizandrin A, Daucosterol, Chrysophanol, Vanillin, Caffeic acid, and Oleanolic acid have been reported to exhibit anti-CRC or anti-cancer effects in previous studies.[38-44] These results suggest that these components may play a crucial role in the therapeutic effectiveness of SIC in treating CRC and warrant further investigation.

Table 2

Details of target proteins for molecular docking.

Target	PBD ID	Resolution	Sequence length	Center coordinates
AKT1	7NH5	1.90 Å	446	14.111, -15.126, -13.203
TP53	1QKT	2.20 Å	248	23.2107.888, -23.841
EGFR	6V60	2.10 Å	370	-2.926, 18.93, -44.158
STAT3	6TLC	2.01 Å	557	-0.822, 31.743, 31.214
TNF	1A8M	2.30 Å	157	20.213, 49.707, 40.959
IL6	1ALU	1.90 Å	186	-0.151, -20.096, 8.967
BCL2	5JSN	2.10 Å	215	15.716, 16.515, 62.513
IL1B	1L2H	1.54 Å	153	10.483, 14.602, 54.84
MYC	6E16	2.40 Å	267	103.452, 79.795, -14.544

Utilizing the previously mentioned active components, we performed target fishing using databases such as TCMSP, SEA, and Swiss Target, eliminating duplicate targets. This effort yielded a total of 317 SJC targets, constituting the "Drug Component-Target" network. We also integrated data from 4 GEO gene chip datasets and collected CRC disease targets from DrugBank, DisGeNET, and TTD databases, removing duplicates, which resulted in 8612 disease targets. By matching and mapping, we identified 276 composite SJC-CRC targets. Next, we created a protein-protein interaction (PPI) network for these composite targets and applied filters based on 3 parameters: Degree Centrality (DC), Betweenness Centrality (BC), and Closeness Centrality (CC). This process resulted in the identification of 20 core target nodes. Among these, there is evidence to suggest that AKT1, TP53, EGFR, STAT3, and TNF are linked to the mechanisms underlying CRC development. These target proteins display higher degree values in the cluster network, indicating their substantial involvement in the therapeutic effects of SIC against CRC and their potential as therapeutic targets.

The analysis of the 276 SJC-CRC intersection targets reveals that GO functional analysis encompasses various biological processes, including proliferation, hypoxia, apoptosis, oxidative stress, and molecular functions such as transcription factors or binding to inflammation-related receptors. These processes are all linked to SJC effects on CRC. Owing to the Warburg effect, CRC tumor tissues frequently display biological phenomena such as hypoxia and glycolysis. Furthermore, the growth and development of CRC cells are influenced by various transcription factors and inflammatory factors. The outcomes of the functional analysis indicate that SIC therapeutic impact on CRC may involve the amelioration of local tissue hypoxia and oxidative stress, as well as the modulation of inflammatory factor activity. However, additional experimental validation is necessary. The KEGG pathway enrichment analysis of the SIC-CRC intersection targets reveals that SJC regulatory effects on CRC predominantly involve signaling pathways related to cancer, immunity, inflammation, proliferation, and apoptosis. These pathways encompass the PI3K-Akt, MAPK, and Chemical carcinogenesis - receptor activation pathways. Previous studies have demonstrated the critical role of the PI3K/AKT/mTOR signaling

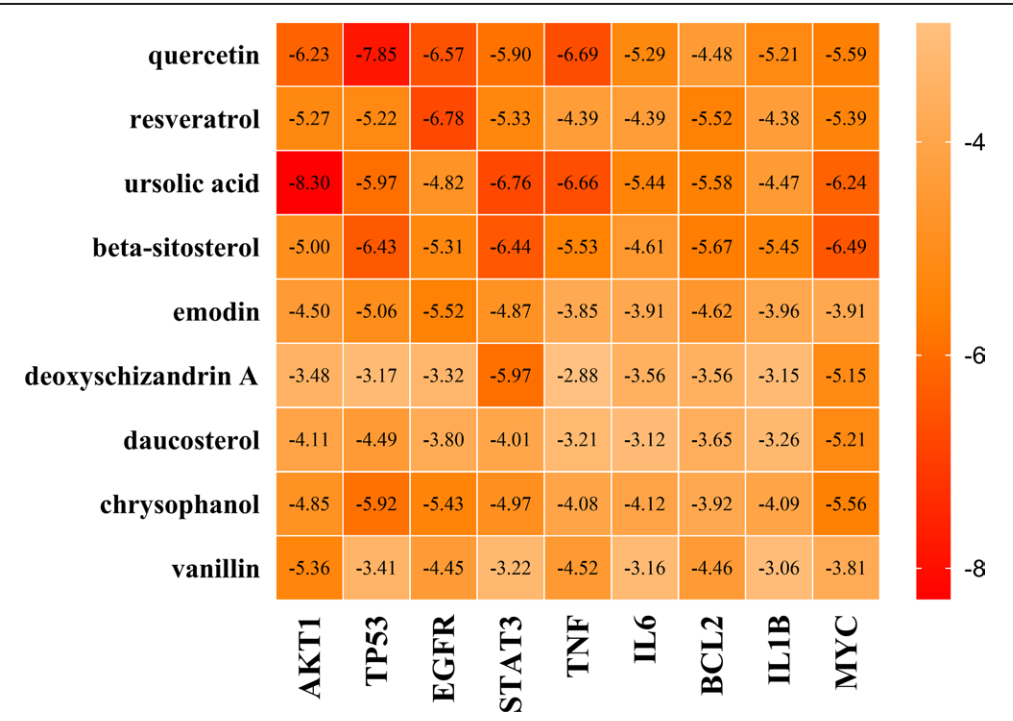


Figure 10. Heat map of molecular docking score. Binding energy(kcal/mol) of key targets and active compounds of herbs.

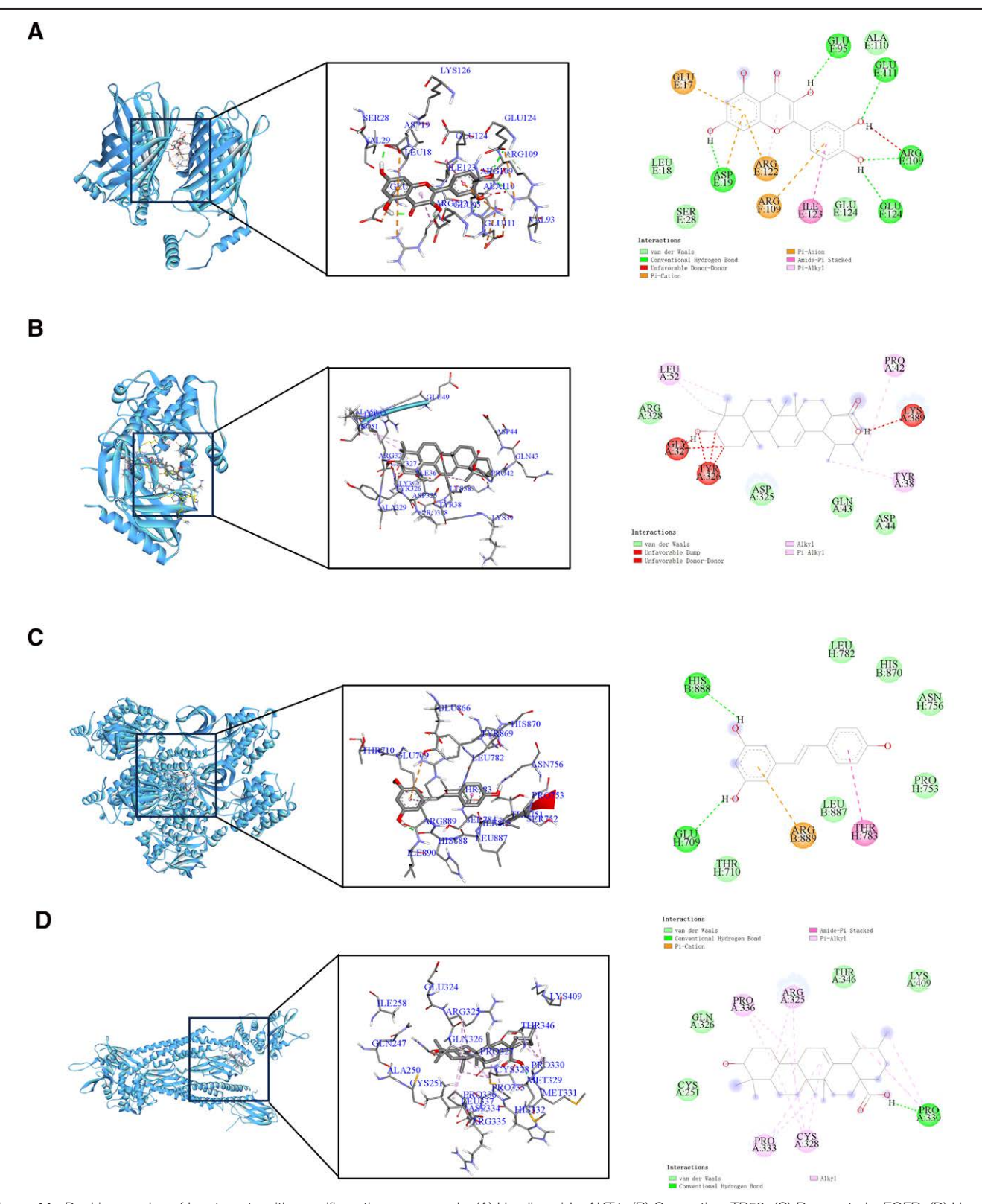


Figure 11. Docking modes of key targets with specific active compounds. (A) Ursolic acid - AKT1, (B) Quercetin - TP53, (C) Resveratrol - EGFR, (D) Ursolic acid - STAT3, (E) Quercetin - TNF, (F) Ursolic acid - IL6, (G) Beta-sitosterol - BCL2, (H) Beta-sitosterol - IL1B, (I) Beta-sitosterol - MYC. On the left are 3-dimensional model views, in the middle are enlarged 3-dimensional model views, and on the right are 2-dimensional views.

pathway in the onset and progression of CRC, encompassing aspects such as proliferation, metastasis, survival, and angiogenesis. [45] For example, Cheng et al provided detailed insights into the inhibitory effects of naringin on CRC cell lines, elucidating that hesperidin, in a dose-dependent manner, arrests CRC cell

proliferation and induces apoptosis by suppressing the PI3K/AKT/mTOR signaling pathway. [46] In vitro studies have shown that betulin can trigger apoptosis, autophagy, and cell cycle arrest in CRC cells by suppressing the activation of the PI3K/AKT/mTOR and MAPK signaling pathways. [47] Furthermore,

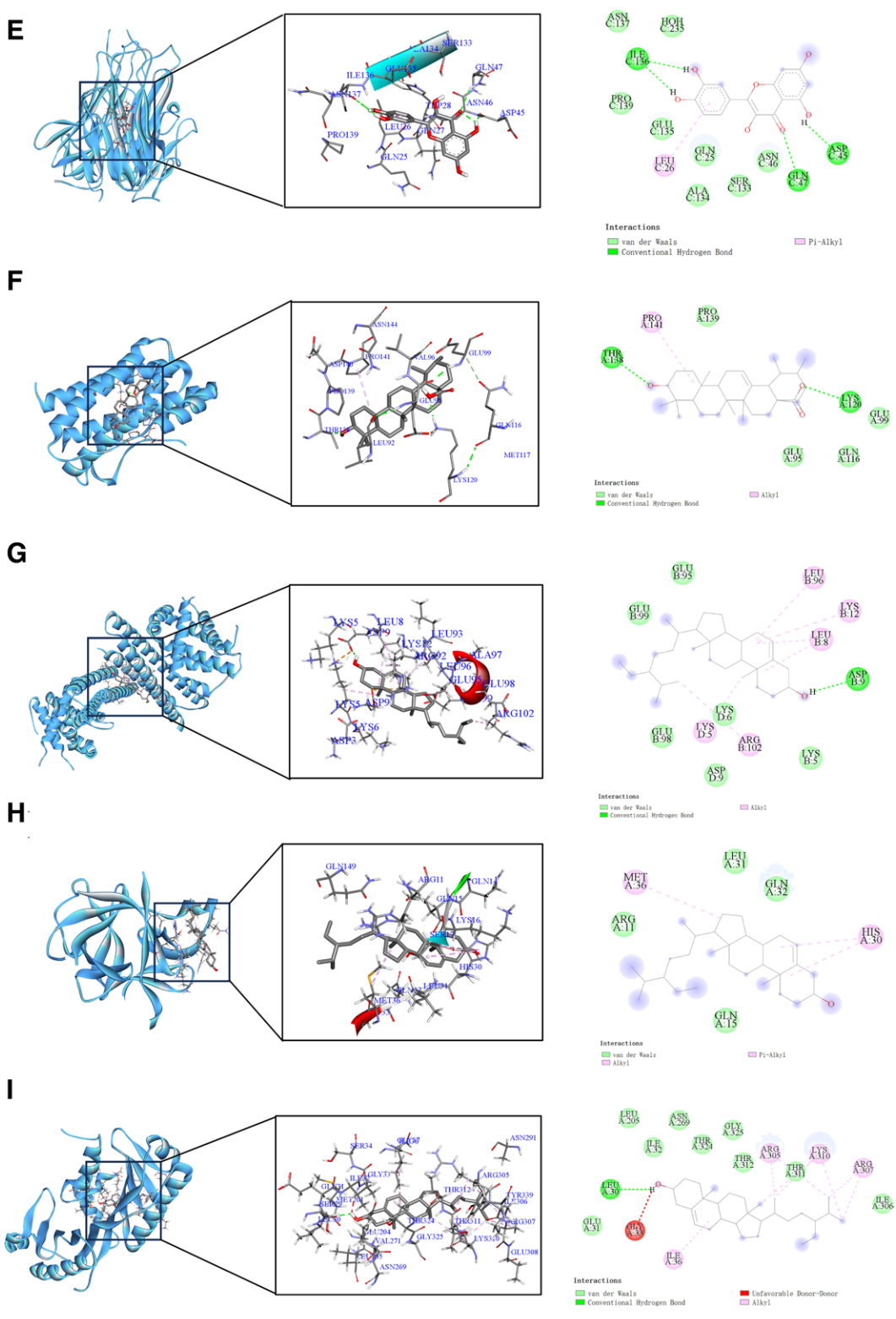


Figure 11. Continued

the aforementioned researchers demonstrated that administering white birch bark extract to a CRC metastasis mouse model significantly reduced lung metastasis of CT26 cells. The 3 major subfamilies of MAPKs—ERK, JNK, and MAPK14—all contribute to the development of CRC. ERK/MAPK plays a pivotal role in the proliferation of cancer cells. [48] Moreover, the MAPK signaling pathway is downstream of numerous growth factor receptors, including EGF, and is activated by various stimuli

such as peptide growth factors, cytokines, hormones, oxidative stress, and endoplasmic reticulum stress.<sup>[49]</sup> This regulation influences the proliferation, differentiation, survival, and apoptosis of CRC cells.<sup>[50]</sup>

We utilized molecular docking to evaluate the binding affinities between the top 9 key target proteins (AKT1, TP53, EGFR, STAT3, TNF, IL6, BCL2, IL1B, and MYC) from the PPI core network and the top 9 active compounds, which include Ursolic

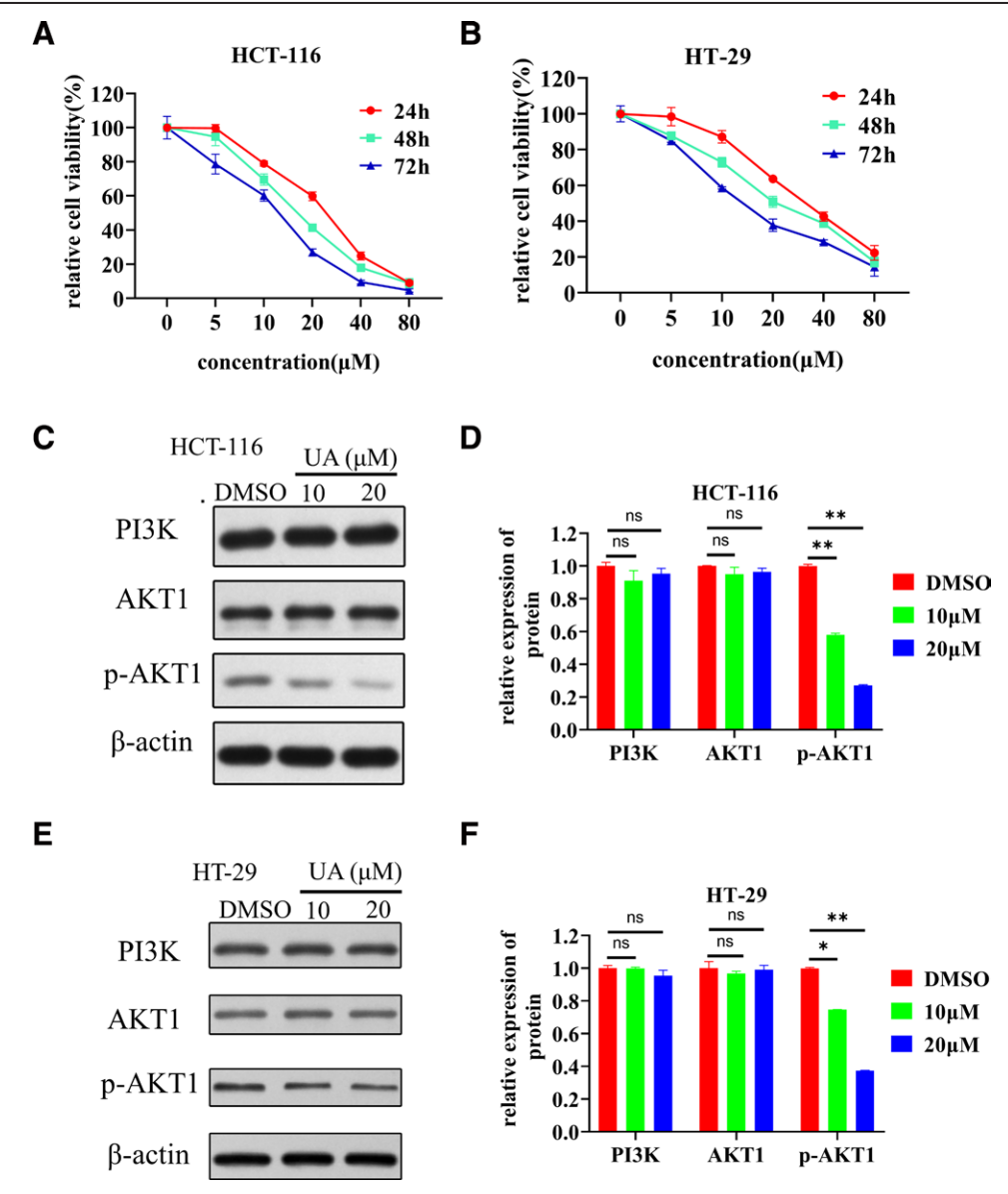


Figure 12. Ursolic acid inhibits CRC cells and the Pl3K/AKT pathway. (A, B) Ursolic acid inhibits the viability of CRC cells as measured by the CCK-8 assay. (C–F) Representative Western blots showing the status and relative expressions of Pl3K, AKT, p-AKT in HCT116 and HT29 cells. β-actin was used as an internal control. UA = Ursolic acid. Values are presented as a mean  $\pm$  SD. \*P < .05, \*\*P < .01 vs control. CCK-8 = cell counting kit-8, CRC = colorectal cancer.

acid, quercetin, resveratrol, beta-sitosterol, emodin, deoxyschizandrin A, daucosterol, chrysophanol, and vanillin. The binding energies observed in the docking results ranged from -2.88 to -8.3 kcal/mol. Typically, binding energies below -4.25 kcal/mol indicate some level of binding activity between the ligand and receptor, while energies below -5.0 kcal/mol suggest a good binding activity, and energies below -7.0 kcal/mol indicate strong binding activity between the ligand and receptor. Of these 9 target proteins, AKT1, TP53, EGFR, and STAT3 displayed the weakest binding affinities. Quercetin, resveratrol, Ursolic acid, and beta-sitosterol demonstrated favorable binding activity with these targets, indicating their potential contribution to SJC therapeutic impact on CRC. Nevertheless, additional in vitro experiments are necessary to validate these predictions.

In vitro experimental results demonstrate that both Ursolic acid and SJC extract reduce p-AKT protein expression without significantly altering PI3K and AKT1 expression. This implies that SJC may depend on its primary active component, Ursolic acid, to inhibit AKT1 phosphorylation after binding to AKT1, aligning with previous research. Zheng et al's study revealed that

Ursolic acid induces apoptosis and mitotic catastrophe in CRC RKO cells by modulating the PI3K/AKT signaling pathway.<sup>[36]</sup> Additionally, there have been reports of Ursolic acid inducing apoptosis in T24 human bladder cancer cells by inhibiting Akt phosphorylation.<sup>[51]</sup> These findings suggest that Ursolic acid, a primary active component in *Salvia chinensis Benth*, may inhibit CRC by suppressing AKT1 activity.

It is essential to acknowledge that this study has specific limitations. Firstly, both the data regarding bioactive compounds and targets were obtained from literature and databases, which means that the reliability and accuracy of predictions rely on the quality of the data. To improve data reliability, employing LC/MS technology for the analysis of bioactive compounds in SJC, as well as conducting metabolomics and pharmacokinetic studies, may offer more precise compound information and pharmacological data. Secondly, this study utilized data mining methods to systematically uncover the mechanisms underlying SJC anti-CRC effects and examined how specific active components modulate core signal pathways in vitro. It crucial to underscore that additional validation through clinical trials and animal experiments

is necessary to substantiate the research findings. Although the predictive results indicate a potential therapeutic effect of SJC on CRC, its actual efficacy needs verification in a clinical context. Conducting clinical trials and animal experiments can furnish additional experimental data to evaluate treatment effectiveness and safety. In summary, this study establishes the foundation for comprehending the potential mechanisms of SJC in the treatment of CRC. Nevertheless, it is imperative to emphasize that further experimental research is imperative to validate and provide additional insights into these findings.

#### 5. Conclusions

In conclusion, this study marks the pioneering use of bioinformatics methodologies, including network pharmacology and molecular docking, for a systematic exploration of the pharmacological and molecular mechanisms underpinning SJC anti-CRC effects. These bioinformatics and computational analyses suggest that quercetin, resveratrol, Ursolic acid, and betasitosterol may serve as the principal bioactive compounds responsible for SJC therapeutic efficacy in CRC. SJC appears to exert its anti-CRC effects through diverse pathways, encompassing PI3K-AKT, MAPK, and TP53, thereby promoting cancer cell apoptosis, curtailing proliferation, and ameliorating pathological damage, inflammation, and oxidative stress. Ursolic acid, a primary active component in Salvia chinensis Benth, may inhibit CRC by suppressing AKT1 activity. In summary, this study delves into the multi-component and multi-pathway regulatory mechanisms of SJC, offering valuable insights into its potential application and further advancement in CRC therapy.

#### **Acknowledgments**

The authors sincerely acknowledge the Prof Qingjiu Ma for some bioinformatics approaches to explore databases.

#### Author contributions

Conceptualization: Zengren Zhao. Formal analysis: Qian Zheng.

Investigation: Xin Wang, Tian Gao, Bingzhou Zhang. Methodology: Qian Zheng, Ning Zhao, Runsen Du.

Software: Qian Zheng. Supervision: Qian Zheng. Validation: Qian Zheng. Visualization: Qian Zheng.

Writing - original draft: Qian Zheng, Ning Zhao, Runsen Du.

Writing - review & editing: Qian Zheng, Zengren Zhao.

#### References

- Sung H, Ferlay J, Siegel RL, et al. Global cancer statistics 2020: GLOBOCAN estimates of incidence and mortality worldwide for 36 cancers in 185 countries. CA Cancer J Clin. 2021;71:209–49.
- [2] Qiu H, Cao S, Xu R. Cancer incidence, mortality, and burden in China: a time-trend analysis and comparison with the United States and United Kingdom based on the global epidemiological data released in 2020. Cancer Commun (Lond). 2021;41:1037–48.
- [3] Zhang Y, Lou Y, Wang J, et al. Research status and molecular mechanism of the traditional Chinese medicine and antitumor therapy combined strategy based on tumor microenvironment. Front Immunol. 2020;11:609705.
- [4] Wang N, Tan H-Y, Chan Y-T, et al. Identification of WT1 as determinant of heptatocellular carcinoma and its inhibition by Chinese herbal medicine Salvia chinensis Benth and its active ingredient protocatech-ualdehyde. Oncotarget. 2017;8:105848–59.
- [5] Jia L, Lin X-R, Guo W-Y, et al. Salvia chinensia Benth induces autophagy in esophageal cancer cells via AMPK/ULK1 signaling pathway. Front Pharmacol. 2022;13:995344.
- [6] Shu G, Zhao W, Yue L, et al. Antitumor immunostimulatory activity of polysaccharides from Salvia chinensis Benth. J Ethnopharmacol. 2015;168:237–47.

- [7] Wang K-N, Hu Y, Han L-L, et al. Salvia chinensis benth inhibits triple-negative breast cancer progression by inducing the DNA damage pathway. Front Oncol. 2022;12:882784.
- [8] Xavier CPR, Lima CF, Pedro DFN, et al. Ursolic acid induces cell death and modulates autophagy through JNK pathway in apoptosis-resistant colorectal cancer cells. J Nutr Biochem. 2013;24:706–12.
- [9] Lin R, Piao M, Song Y, et al. Quercetin Suppresses AOM/DSS-induced colon carcinogenesis through its anti-inflammation effects in mice. J Immunol Res. 2020;2020:9242601.
- [10] Brockmueller A, Buhrmann C, Shayan P, et al. Resveratrol induces apoptosis by modulating the reciprocal crosstalk between p53 and Sirt-1 in the CRC tumor microenvironment. Front Immunol. 2023;14:1225530.
- [11] Zhang R, Zhu X, Bai H, et al. Network pharmacology databases for traditional Chinese medicine: review and assessment. Front Pharmacol. 2019;10:123.
- [12] Li S, Zhang B. Traditional Chinese medicine network pharmacology: theory, methodology and application. Chin J Nat Med. 2013;11:110–20.
- [13] Suhail Y, Cain MP, Vanaja K, et al. Systems Biology of Cancer Metastasis. Cell Syst. 2019;9:109–27.
- [14] Nogales C, Mamdouh ZM, List M, et al. Network pharmacology: curing causal mechanisms instead of treating symptoms. Trends Pharmacol Sci. 2022;43:136–50.
- [15] Lin F, Zhang G, Yang X, et al. A network pharmacology approach and experimental validation to investigate the anticancer mechanism and potential active targets of ethanol extract of Wei-Tong-Xin against colorectal cancer through induction of apoptosis via PI3K/AKT signaling pathway. J Ethnopharmacol. 2023;303:115933.
- [16] Schloss J, Ryan K, Steel A. Corrigendum to A randomised, double-blind, placebo-controlled clinical trial found that a novel herbal formula UROX® BEDTIME BUDDY assisted children for the treatment of nocturnal enuresis Phytomedicine (2021) 153783. Phytomedicine. 2022;99:153992.
- [17] Pinzi L, Rastelli G. Molecular docking: shifting paradigms in drug discovery. Int J Mol Sci. 2019;20:4331.
- [18] Ru J, Li P, Wang J, et al. TCMSP: a database of systems pharmacology for drug discovery from herbal medicines. J Cheminform. 2014;6:13.
- [19] Chen CY-C. TCM Database@Taiwan: the world's largest traditional Chinese medicine database for drug screening in silico. PLoS One. 2011;6:e15939.
- [20] Zhou W, Zhang H, Wang X, et al. Network pharmacology to unveil the mechanism of Moluodan in the treatment of chronic atrophic gastritis. Phytomedicine. 2022;95:153837.
- [21] Keiser MJ, Roth BL, Armbruster BN, et al. Relating protein pharmacology by ligand chemistry. Nat Biotechnol. 2007;25:197–206.
- [22] Daina A, Michielin O, Zoete V. SwissTargetPrediction: updated data and new features for efficient prediction of protein targets of small molecules. Nucleic Acids Res. 2019;47:W357–64.
- [23] Piñero J, Saüch J, Sanz F, et al. The DisGeNET cytoscape app: exploring and visualizing disease genomics data. Comput Struct Biotechnol J. 2021;19:2960–7.
- [24] Wishart DS, Feunang YD, Guo AC, et al. DrugBank 50: a major update to the DrugBank database for 2018. Nucleic Acids Res. 2018;46:D1074–82.
- [25] Li YH, Yu CY, Li XX, et al. Therapeutic target database update 2018: enriched resource for facilitating bench-to-clinic research of targeted therapeutics. Nucleic Acids Res. 2018;46:D1121–7.
- [26] UniProt: the universal protein knowledgebase in 2021. Nucleic Acids Res. 2021;49:D480–9.
- [27] Szklarczyk D, Gable AL, Nastou KC, et al. The STRING database in 2021: customizable protein-protein networks, and functional characterization of user-uploaded gene/measurement sets. Nucleic Acids Res. 2021;49:D605–12.
- [28] Ferreira LG, Dos Santos RN, Oliva G, et al. Molecular docking and structure-based drug design strategies. Molecules. 2015;20:13384–421.
- [29] Liu J, Liu J, Tong X, et al. Network pharmacology prediction and molecular docking-based strategy to discover the potential pharmacological mechanism of Huai Hua San against ulcerative colitis. Drug Des Devel Ther. 2021;15:3255–76.
- [30] Dekker E, Tanis PJ, Vleugels JLA, et al. Colorectal cancer. Lancet. 2019;394:1467–80.
- [31] Cao W, Chen H-D, Yu Y-W, et al. Changing profiles of cancer burden worldwide and in China: a secondary analysis of the global cancer statistics 2020. Chin Med J (Engl). 2021;134:783–91.
- [32] Li C, Sun Y-D, Yu G-Y, et al. Integrated omics of metastatic colorectal cancer. Cancer Cell. 2020;38.
- [33] Zielińska A, Włodarczyk M, Makaro A, et al. Management of pain in colorectal cancer patients. Crit Rev Oncol Hematol. 2021;157:103122.

- [34] Xiang Y, Guo Z, Zhu P, et al. Traditional Chinese medicine as a cancer treatment: modern perspectives of ancient but advanced science. Cancer Med. 2019:8:1958–75.
- [35] Brockmueller A, Shayan P, Shakibaei M. Evidence that β1-integrin is required for the anti-viability and anti-proliferative effect of resveratrol in CRC cells. Int J Mol Sci. 2022;23:4714.
- [36] Zheng J-L, Wang S-S, Shen K-P, et al. Ursolic acid induces apoptosis and anoikis in colorectal carcinoma RKO cells. BMC Complement Med Ther. 2021;21:52.
- [37] Wang Z, Zhan Y, Xu J, et al. β-Sitosterol reverses multidrug resistance via BCRP suppression by inhibiting the p53-MDM2 interaction in colorectal cancer. J Agric Food Chem. 2020;68:3850–8.
- [38] Zhang Y, Pu W, Bousquenaud M, et al. Emodin inhibits inflammation, carcinogenesis, and cancer progression in the AOM/DSS model of colitisassociated intestinal tumorigenesis. Front Oncol. 2020;10:564674.
- [39] Zhou Z, Wang Y, Ji R, et al. Vanillin derivatives reverse fusobacterium nucleatum-induced proliferation and migration of colorectal cancer through E-Cadherin/β-Catenin pathway. Front Pharmacol. 2022;13:841918.
- [40] Chen C, Kuo Y-H, Lin C-C, et al. Decyl caffeic acid inhibits the proliferation of colorectal cancer cells in an autophagy-dependent manner in vitro and in vivo. PLoS One. 2020;15:e0232832.
- [41] Li L, Lin J, Sun G, et al. Oleanolic acid inhibits colorectal cancer angiogenesis in vivo and in vitro via suppression of STAT3 and Hedgehog pathways. Mol Med Rep. 2016;13:5276–82.
- [42] Han B, Jiang P, Liu W, et al. Role of daucosterol linoleate on breast cancer: studies on apoptosis and metastasis. J Agric Food Chem. 2018;66:6031–41.

- [43] Lim W, An Y, Yang C, et al. Chrysophanol induces cell death and inhibits invasiveness via mitochondrial calcium overload in ovarian cancer cells. J Cell Biochem. 2018;119:10216–27.
- [44] Xu S-Y, Su H, Zhu X-Y, et al. Long-circulating doxorubicin and schizandrin A liposome with drug-resistant liver cancer activity: preparation, characterization, and pharmacokinetic. J Liposome Res. 2022;32:107–18.
- [45] Stefani C, Miricescu D, Stanescu-Spinu I-I, et al. Growth factors, PI3K/ AKT/mTOR and MAPK signaling pathways in colorectal cancer pathogenesis: where are we now? Int J Mol Sci. 2021;22:10260.
- [46] Cheng H, Jiang X, Zhang Q, et al. Naringin inhibits colorectal cancer cell growth by repressing the PI3K/AKT/mTOR signaling pathway. Exp Ther Med. 2020;19:3798–804.
- [47] Han Y-H, Mun J-G, Jeon HD, et al. Betulin inhibits lung metastasis by inducing cell cycle arrest, autophagy, and apoptosis of metastatic colorectal cancer cells. Nutrients. 2019;12:66.
- [48] Fang JY, Richardson BC. The MAPK signalling pathways and colorectal cancer. Lancet Oncol. 2005;6:322–7.
- [49] Kim EK, Choi E-J. Compromised MAPK signaling in human diseases: an update. Arch Toxicol. 2015;89:867–82.
- [50] Sun H, Ou B, Zhao S, et al. USP11 promotes growth and metastasis of colorectal cancer via PPP1CA-mediated activation of ERK/MAPK signaling pathway. EBioMedicine. 2019;48:236–47.
- [51] Gai L, Cai N, Wang L, et al. Ursolic acid induces apoptosis via Akt/ NF-κB signaling suppression in T24 human bladder cancer cells. Mol Med Rep. 2013;7:1673–7.